

# SPACE SCIENCES LABORATORY

CASE FILE  
COPY

N 70 15493  
NASA CR 107559

Final Report

COMPLETION OF DESIGN AND FABRICATION OF A  
ROCKET PAYLOAD FOR SEARCH OF THE SOUTHERN HEMISPHERE SKY  
FOR GALACTIC X-RAY SOURCES

Supported by

NASA Contract  
NSR 09-005-056

<sup>6</sup>  
NSR-05-003-287

UNIVERSITY OF CALIFORNIA, BERKELEY

The Catholic University of America  
Washington, D.C. 20017

Final Report

COMPLETION OF DESIGN AND FABRICATION OF A  
ROCKET PAYLOAD FOR SEARCH OF THE SOUTHERN HEMISPHERE SKY  
FOR GALACTIC X-RAY SOURCES

Supported by

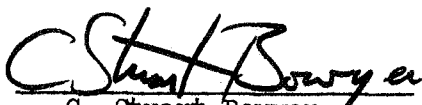
NASA Contract  
NSR 09-005-056

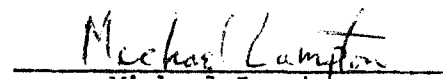
Submitted to:

Office of Grants and Research Contracts  
National Aeronautics and Space Administration  
Washington, D. C.

Prepared at:

The University of California  
Space Sciences Laboratory  
Berkeley, California

  
C. Stuart Bowyer  
Principal Investigator

  
Michael Lampton  
Co-Investigator



## Introduction

This report covers the development of an Aerobee payload and other instrumentation for studies in galactic x-ray astronomy. This work was begun at Catholic University of America in Washington D.C. and was completed at the University of California at Berkeley. This report describes the instrumentation developed through launch.

This report is intended to complete the reporting requirements for NASA Contract NSR 09-005-056 to the Catholic University of America and NASA Contract NSR 05-003-287 to the University of California at Berkeley. It has been submitted in duplicate with only the front cover changed since the contract to the University of California was awarded to complete the development of the payload begun at the Catholic University of America. The primary emphasis of this report has been placed on those parts which represented new developments.

The development of a second Aerobee instrumentation package at the University of California and an analysis of the results obtained with both payloads will be described in a separate report.

## Instrumentation Developed

Three areas of instrumentation development were supported by these two contracts.

- A. The development of an Aerobee instrumentation package for galactic X-ray astronomy.
- B. The development of an instrument designed to carry out galactic X-ray astronomy from a balloon. This instrument consists of 1) a stabilized balloon gondala with a polar axis telescope mount capable of pointing a

300 lb X-ray telescope at any position in the sky to an accuracy better than a degree and 2) an X-ray telescope with over 2000 cm<sup>2</sup> collecting area.

- C. The development of a far UV photometer for use in the wavelength band from 100 to 1000 Å. This instrument was employed in two areas of research 1) a search for XUV resonant radiation in the earth's geocorona and 2) a search for XUV radiation from objects in the night sky. In addition, as work on this instrumentation progressed it became clear that it provided a powerful tool for analyzing planetary atmospheres. This instrument was proposed for a Flyby to Jupiter and a Flyby to Venus/Mercury. Although another group was chosen for the Jupiter flyby mission, they have decided to employ instrumentation similar to that developed by us. As a consequence, it can be fairly said that our efforts contributed directly to the instrumentation which will fly on the Jupiter Flyby mission.

A. Development of an Aerobee Instrumentation Package.

1. The Overall System

This payload was designed to 1) search for new X-ray point sources in the night sky and determine their spectrum, and 2) to examine the intensity and spacial distribution of the diffuse sky background. The primary emphasis was to be placed on the softer X-ray energies.

The primary problems to be overcome were the low ratio of signal to noise at the lower X-ray energies and the uncertain background subtractions which had been employed in previous work. The signal to noise problem was to be approached in two ways 1) by increasing the collecting area to the

maximum possible and 2) by employing a complete wraparound gas anticoincidence counter on all detectors. The background subtraction was to be handled by flying a second counter almost identical with the first as far as particle background effects but which was essentially opaque to X-rays.

The overall size of the counters was determined by the size of the maximum length of an Aerobee payload. The following analysis was carried out to determine the optimum relative sizes for the signal and background counter.

If an observation is made of both a signal and background for a time  $T_1$ , the number of counts observed,  $n_1$ , is related to the true signal,  $S$ , and true background,  $B$ , by the relation

$$n_1 = ST_1 + BT_1 \pm \sqrt{\sigma_s^2 + \sigma_B^2}$$

where  $\sigma$  is the rms deviation and is given by

$$\sigma_s = \sqrt{ST_1}$$

$$\sigma_{B_1} = \sqrt{BT_1}$$

If the background is then measured alone, one obtains a second observational number,  $n_2$ , independent of the first given by

$$n_2 = B T_2 \pm \sigma_{B_2}$$

Now to calculate the signal,  $s$ , as estimated from the experimental evidence (note it will only approximate the true signal,  $S$ ) we subtract giving

$$s = \frac{n_1}{T_1} - \frac{n_2}{T_2}$$

$$= \frac{ST_1}{T_1} \pm \sqrt{\frac{\sigma_S^2}{T_1^2} + \frac{\sigma_{B_1}^2}{T_1^2} + \frac{\sigma_{B_2}^2}{T_2^2}}$$

where the standard deviations add because the two measurements are independent.

If the total observing time  $T$  is fixed, then  $T_1 + T_2 = T$ . We now find that  $T$  which minimizes the error in  $s$  by finding

$$\frac{ds}{dT_1} = 0$$

This gives us the relation

$$S + B = \frac{BT_1^2}{(T - T_1)^2}$$

If  $S = n B$  we find

$$T_1 = \sqrt{n+1} T_2$$

In table I we have computed this for a number of representative values of  $n$ .

Table I  
Optimum Observing Time for Various Ratios  
of Signal to Background

$S \ll B$	$T_S = T_B$
$S = B/2$	$T_S = 1.2 T_B$
$S = B$	$T_S = 1.4 T_B$
$S = 5B$	$T_S = 2.2 T_B$
$S = 10B$	$T_S = 3.1 T_B$

In an actual Aerobee flight, of course, the signals obtained from point sources are compared with a nearby background which is supposedly source free. The observed background signal, however, is composed of true X-ray background plus a charged particle background which has escaped detection by the anticoincidence counters. The observing time for each of these two components will be the same. In this case the free parameter to be varied to optimize the measurement of the true X-ray background is not the ratio of the observing times but is the ratio of the areas of the charged particle and the X-ray detector. Since anticoincidence counters are ordinarily about 90% effective, we see from Table I that the X-ray counter area should be about three times the area of the background detector. It was decided to divide the X-ray counter into two separate units to increase the likelihood of obtaining at least some data in the case of a partial failure in the instrumentation.

The payload was to be free spinning and hence an aspect solution would be required. Two stellar photometers were employed to obtain aspect data. Two far UV photometers (described in a later section of this report) were also designated as part of the instrumentation for this flight.

A block diagram of the instrumentation section as described is shown in Figure I.

## 2. Proportional counter systems

As a result of the arguments outlined in section 1, the source counters to be employed were approximately 50% longer than those we had employed previously. Two potential problem areas were examined, the stability of the anode wires in long counters and the detector doors and their release mechanism.



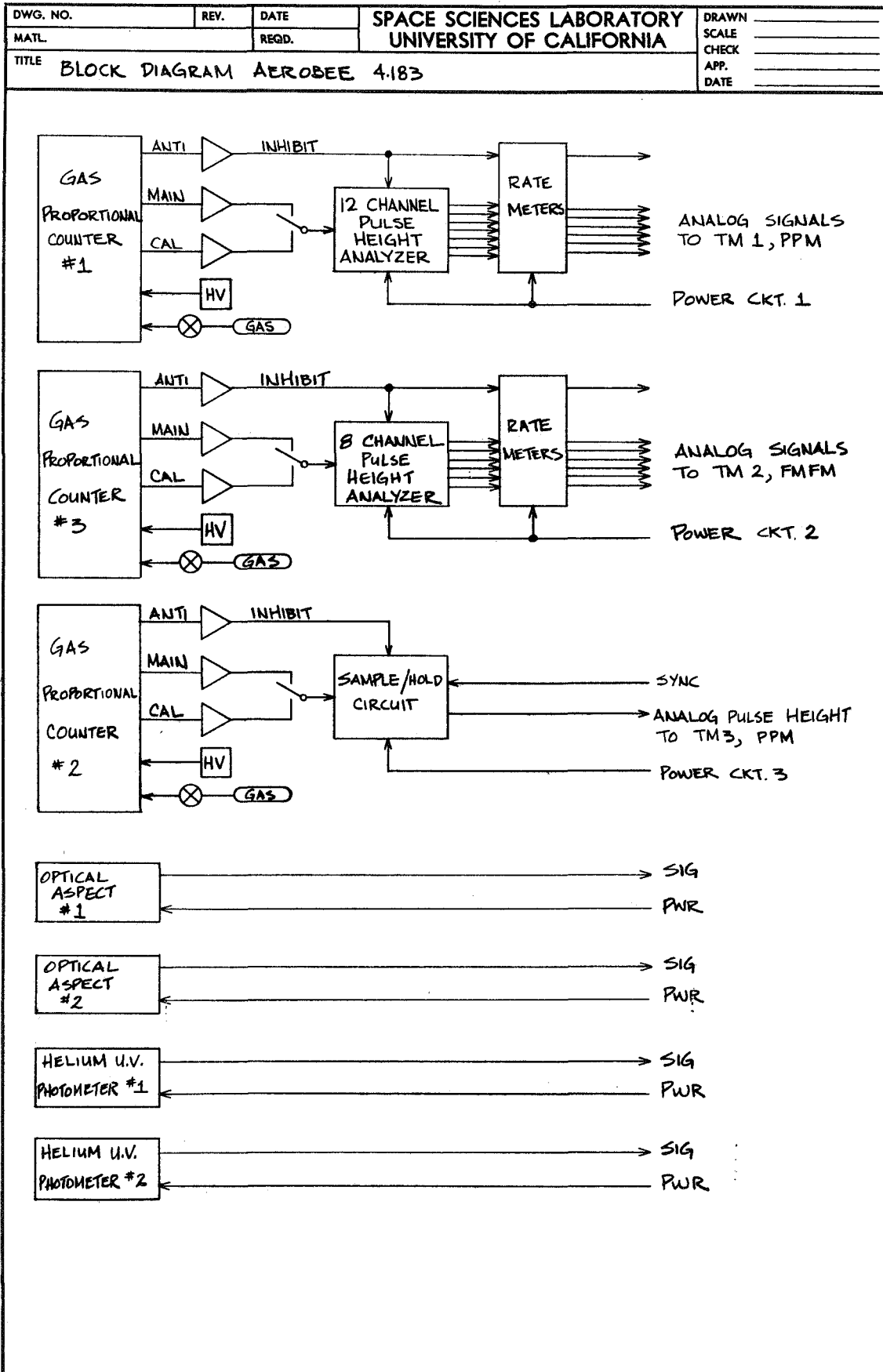


Figure 1. Block diagram of the instrumentation section.

The stability of the anode wire was investigated by fabricating test counters of various lengths. These were subjected to a vibration check to Aerobee specifications. Observation of the units was carried out with aid of a synchronous light. It was established that the anode wires in counters of the length to be employed underwent sufficient lateral displacement to strike the walls of window of the detector. Consequently, a center support would be required for the anode wires in these large detectors.

The detector door was provided with additional door stiffeners for extra strength. The door release mechanism used in previous flights was evaluated and considered to be satisfactory. Unfortunately, it was later established that the mechanism was only marginally acceptable for this length door.

The proportional counter system itself was similar to that employed on our previous flight. In brief, it employed a gas flow system with flow commencing one hour before launch and continuing through the flight. Gas was provided on the ground via an umbilical and in flight from a gas bottle. Each of the three counters was provided with an independent gas supply and control network for redundancy.

A variety of data processing systems were considered for this flight. In our previous flight we had employed an onboard stacked discriminator pulse height analyser with integrating ratemeter outputs. This system had the advantage of availability and flight proven reliability. It had a number of disadvantages. It was relatively difficult to change the level settings of the discriminators. The stacked discriminator approach was reaching its practical limit with twelve channels of energy discrimination. This was not important in the case of a spinning rocket because in this

case the data would be signal limited but nonetheless it clearly was a device with a limited future. The use of integrating ratemeters was advantageous for systems checks because the data is easily interpreted on an oscilloscope. However, the flight data must be hand processed. Again this was not a problem for this flight but indicated a limited usefulness for the future.

A second approach evaluated was the use of a height to time pulse height analyser with digital storage. This system can be expanded to give as much energy resolution as desired and provides the data in a form compatible with machine processing. Its disadvantages are that it is rather bulky, it uses a fair amount of power, and time resolution is lost.

A third approach considered was pulse stretching and readout of the entire pulse. This system is clearly a device of the past because of its low data handling capability. Moreover, most of what is transmitted is not information but concerns the shape of the pulse. This consideration lead us to develop a "sample and hold" circuit (described below) which in effect presents only the information part of the pulse, its magnitude, to the telemetry system.

It was decided on the basis of rapid time response and proven reliability to employ stacked discriminator pulse height analysers with integrating rate meter outputs on two of the three counters in this rocket. The sample and hold circuit would be employed on the third counter. On the second rocket where the scan rate would be over an order of magnitude slower and the time response would not be critical, a height to time pulse height analyser with digital storage and output would be employed.

In Figure 2 is a schematic of the stacked discriminator circuit employed. This is the eight channel unit, the twelve channel unit is identical except for the number of discriminators.

In Figure 3 is shown the "sample and hold" data processing unit. Because of its potential usefulness, we will describe it in some detail. We expect to publish an account of this circuit in the literature shortly. The basic features of this circuit is that the time of occurrence of the transient signal need not be known in advance: the presence of a signal greater than a certain threshold causes the peak value of the signal to be stored, and also causes any further signals to be rejected until the stored signal is transmitted. This circuit is, then, appropriate for transmission of (nearly) real-time X-ray signals through periodically sampled analog links such as the GSFC pulse-position modulation system.

The circuit consists of two subsystems. The analog subsystem is a linear gate Q1-Q4, a storage capacitor, and a voltage follower. Its function is to sample and hold any signal upon command. The digital subsystem consists of a threshold comparator and two flip flops. Its function is to generate the sample command upon receipt of an acceptable signal, and to allow no further samples until after the stored signal has been telemetered.

In operation, the delayed signal is applied simultaneously to the linear gate, which is normally off, and to the threshold comparator. With the component values shown in Figure 3 a minimum signal of approximately 0.1 volt is needed to clock the BUSY flipflop. The logic arrangement of this flipflop is such as to place it in a "1" state upon being clocked; further clock signals cannot then cause any change of state. Following the



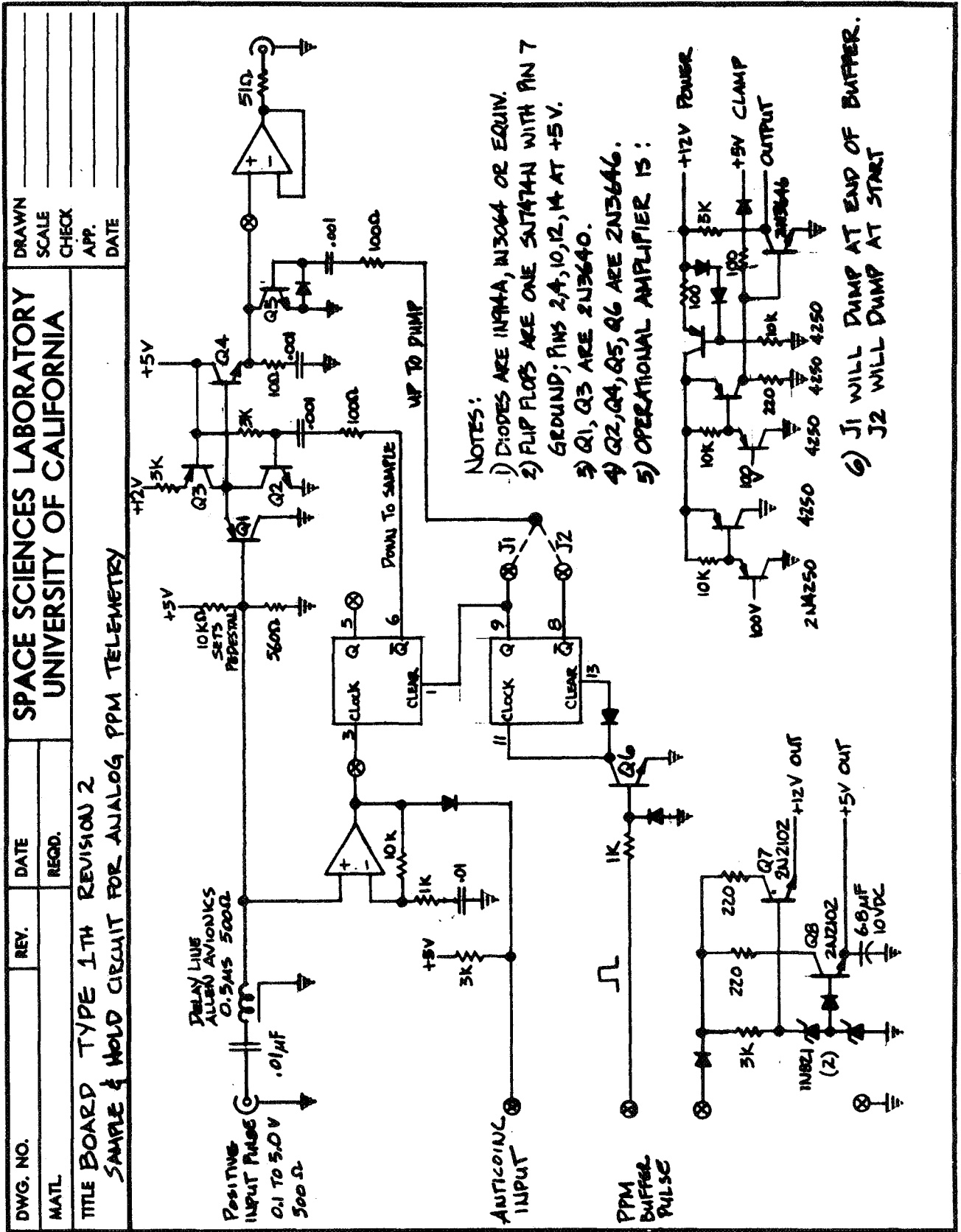


Figure 3. Sample and hold data processing unit.

transition of the BUSY flipflop to a logical "1", the linear gate is enabled for approximately 2  $\mu$ sec and the peak value of whatever signal is present appears at the emitter of Q4, i.e. at the storage capacitor.

Note that loading of this storage capacitor will not occur if the "anticoincidence" inhibit wire is held grounded, or if the telemetry system is reading the stored voltage. In the first case, the BUSY flipflop will not be clocked, while in the second case that flipflop will be held in the CLEAR condition.

The function of the PPM buffer signal is to provide an indication of the time at which telemetry readings are taken. Upon receipt of a PPM pulse, the BUSY flipflop is cleared, and also the storage capacitor is briefly short-circuited by transistor Q5.

One further feature of this circuit is the presence of a pedestal or d.c. offset which is added to each successfully sampled pulse. Its purpose is to lift even very small signal voltages out of the range of noise fluctuations of the telemetry system. It thus avoids confusion of telemetry noise with small X-ray signals. The actual pulse heights are calculated during post-flight data reduction by subtracting the constant pedestal voltage from each sample voltage.

Because time elapses between loading and reading the storage capacitor, a voltage error proportional to that time interval appears:

$$\Delta V = \dot{V} \Delta t = \frac{I}{C} \Delta t$$

Here, I represents the sum of the currents which flow through the storage capacitor C. The design described here has  $I \approx 10^{-7}$  amp and  $C = 10^{-9}$  farad. The elapsed time  $\Delta t$  is random but never exceeds 50  $\mu$ sec, so that  $|\Delta V| \leq 5$  mV.

In Figure 4 the response of this circuit to input signals between 0 and 6 volts amplitude has been plotted. Signal pulses having a rise time of 100  $\mu$ sec and a fall time of 1  $\mu$ sec were generated by a RIDL 47-2 mercury pulser. The samples were telemetered via PPM to a nearby ground station and provided the input-output relationship shown. The random errors were found to be no larger than the 17 mV digitizing interval of the ground station equipment.

The rate at which events can be telemetered by a system of this kind is limited by the PPM sampling rate. Suppose that the events occur independently of each other with some mean rate  $M$ . Then the probability that in time  $T$  exactly  $N$  events will have occurred is given by Poisson's formula

$$P(N) = e^{-TM} \frac{(TM)^N}{N!}$$

Now the telemetry system described here ignores pulses beyond the first one in each time interval  $T$ , and so  $P(1)$ ,  $P(2)$ , ...etc. are not separately measured. However  $P(0)$  is precisely measured; it is exactly the fraction of samples which contain no pulse:

$$P(0) = e^{-TM}$$

which permits the calculation of the true mean rate  $M$ :

$$M = \frac{1}{T} \ln \frac{1}{P(0)} = \frac{1}{T} \ln \frac{1}{1 - RT}$$

Here, the observed count rate is represented by  $R$ .



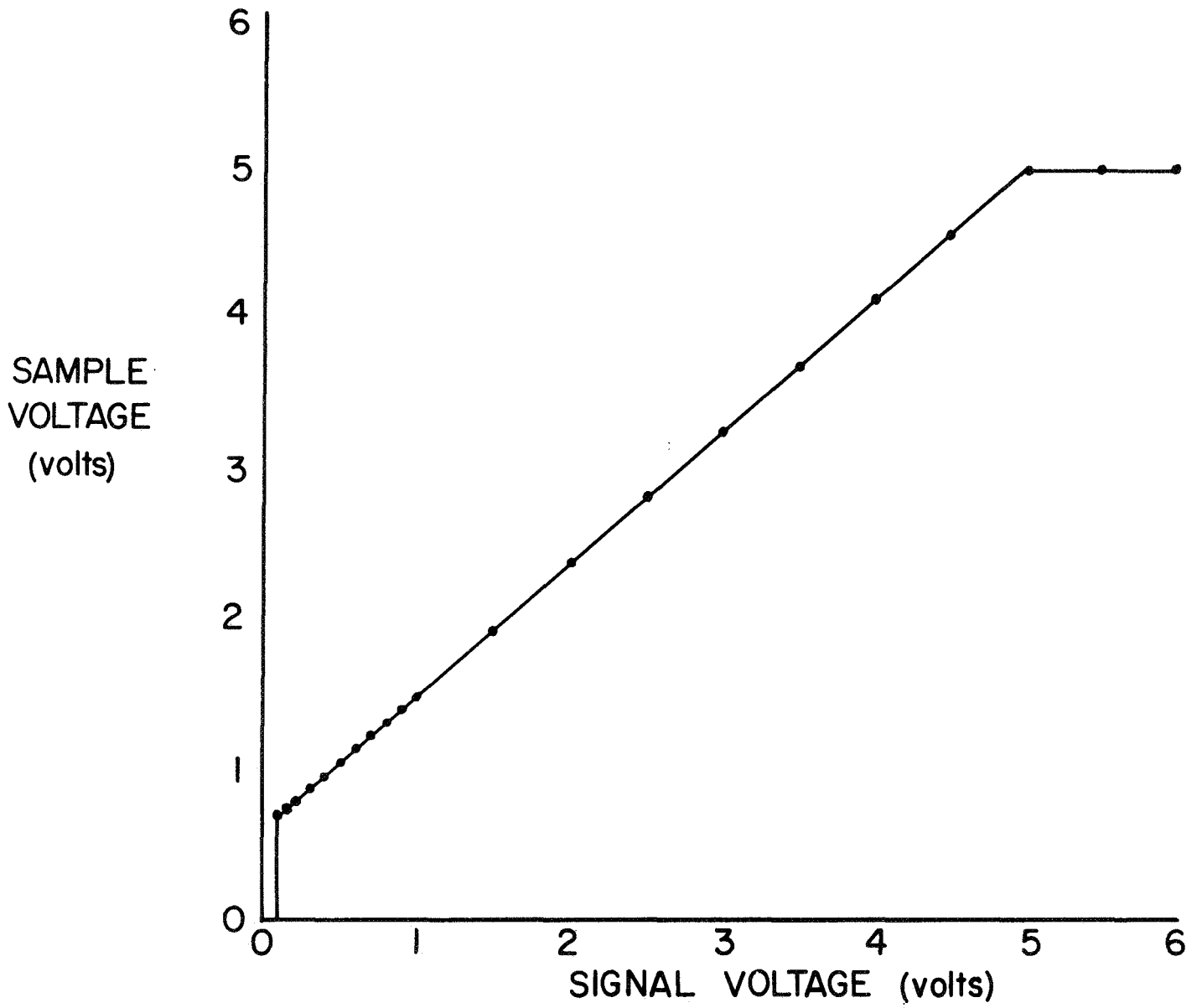


Figure 4. Response of the sample and hold circuit to a varying input signal

Modification of these formulas is necessary when there are additional causes of dead time, as is the case here. The nonzero width of the PPM timing signal (approx. 1  $\mu$ sec) and the occasional rejection of valid signals by the anticoincidence circuit (approximately 10  $\mu$ sec loss, 100 times per second) act to reduce the observed count rate R. If each accumulation is shortened by a factor f, then the observed rate

$$R = \frac{1}{T} (1 - f e^{-fMT})$$

from which the calculated true mean rate M is

$$M = \frac{1}{ft} \ln \frac{1}{1 - RT}$$

In Figure 5 the relationship between the fraction of counts transmitted or average live time R/M and the true mean rate M is graphed. For this calculation, a fixed dead time of 1  $\mu$ sec per sample plus 10  $\mu$ sec per anticoincidence event was assumed.

### 3. Optical Aspect Photometer

As a consequence of a previous unfortunate experience our group had with such items, it was decided that at least one of the two photometers employed on this flight would be one which had a long history of flight success. The only photometer which met this criteria was one manufactured by the American Science and Engineering Corporation. This unit was viewed as unbelievably expensive but was purchased nonetheless on the basis that the flight depended critically on the successful operation of the aspect photometer. Development of a unit of our own was also begun.

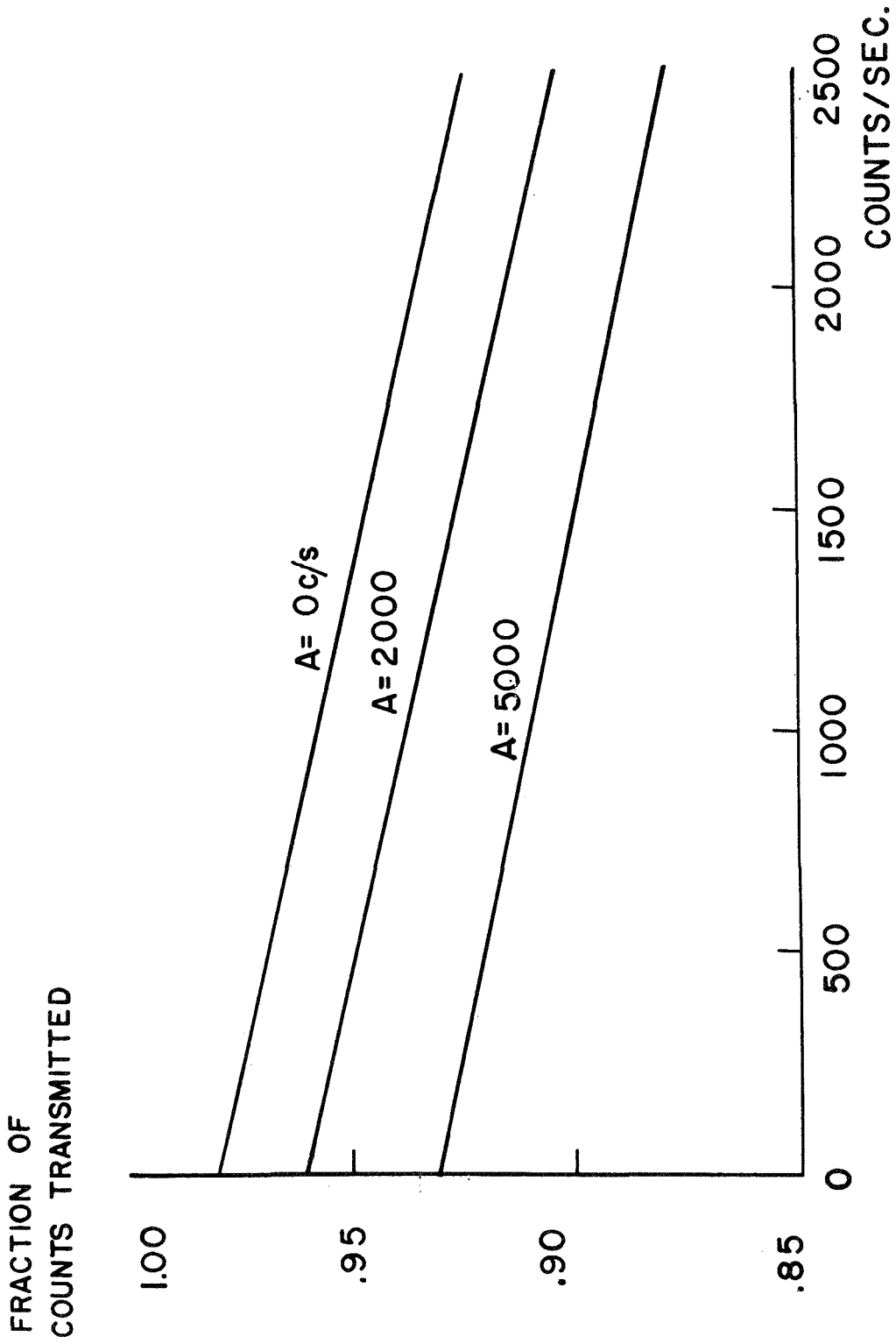


Figure 5. Fraction of counts transmitted vs. true count rate with three background rates  $A$ .

A block diagram of the photometer developed is shown in Figure 6. The optical train begins with a one inch achromatic lens which was shock mounted in a teflon bushing. The entire lens unit was mounted in an adjustable assembly. This assembly was varied to provide optimum focusing of stellar signals on the focal plane slit. Optical baffling was provided between the objective lens and this slit. The photomultiplier employed, an RCA C31016A, is an extremely small ruggedized tube with a bialkalide photocathode. The dynode chain for the tube and a preamplifier board were encapsulated as a single unit.

The optical train, a high voltage supply, a power converter and a discriminator and ratemeter board were all mounted in a magnesium box measuring  $2\frac{1}{2}$ " x  $2\frac{1}{2}$ " x 6". For maximum strength this box was fabricated out of a single block of magnesium. The entire assembly weighted 1.1 lbs. In comparison, the commercial unit purchased was over three times as large and over twice as heavy.

#### 4. Test and Evaluation

All systems were subjected to the usual array of preflight checks at the University of California. In particular all units employing high voltage were subjected to at least six rapid pumpdown vacuum corona checks and at least two pumpdowns of over an hour each. The optical aspect sensors were first checked for optical response at the University of California Leushner Observatory in Lafayette. When ambiguous results were obtained because of the relatively bright sky background at this location, these units were rechecked at the site of the Lick Observatory on Mt. Hamilton.

DWG. NO.	REV.	DATE	SPACE SCIENCES LABORATORY UNIVERSITY OF CALIFORNIA	DRAWN
MATL.	REQD.			SCALE
TITLE			PHOTOMETER TYPE 3 BLOCK DIAGRAM	CHECK
				APP.
				DATE

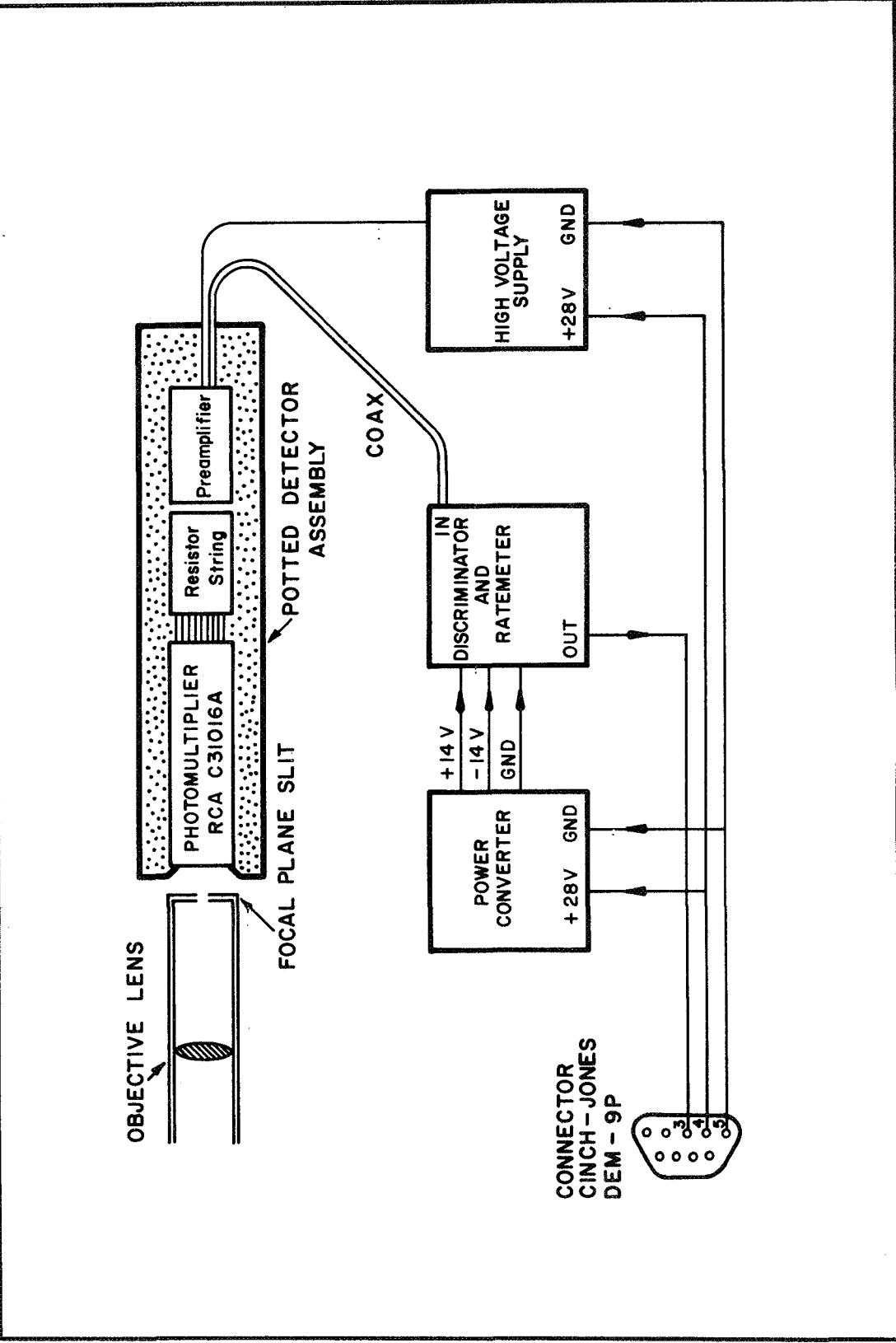


Figure 6. Optical aspect photometer block diagram.

The instrumentation section was shipped to GSFC for integration, test and evaluation. During these tests, two failures occurred. First, the AS&E optical aspect sensor failed. An attempt was made to obtain a replacement unit but in spite of an extensive effort on the part of AS&E, we were unable to obtain a working photometer. Ultimately, we sent our mechanical engineer to Boston to work with AS&E on this effort and a makeshift, though flightworthy, photometer was produced. The second failure during T&E concerned the door release mechanism on one of the two long counter doors. This mechanism failed to operate after heating which simulated the effects of atmospheric friction on the rocket skin. A thermal shield was added to the door and the release mechanism was modified slightly. Subsequently, the mechanism was fired three times in thermal-vac with complete success.

Flight readiness checks at the launch site included the usual array of preflight tests. In addition, all units employing high voltages were again checked for vacuum breakdown.

## 5. Flight

The rocket and Goddard support instrumentation performed as expected. In our instrumentation section, however, a door covering on one of the X-ray source counters failed to deploy. Although this counter operated satisfactorily throughout the flight, it provided no useful data. The second source counter provided data for a portion of the flight until one channel of its associated anticoincidence counter began to provide an anomalously high count. This effectively blocked out this counter for the remainder of the flight. As a consequence of

these two failures the experiment was comprimized to the extent that the primary goals of the mission were not met. It is interesting (and sad) to note that of the nine possible counter combinations in which these two failures could have occurred, only this particular combination could have so completely comprimized the flight. On the brighter side, however, data was obtained on two X-ray sources. This data is currently being analysed.

All the remaining instrumentation operated as planned. In particular, the optical aspect photometer developed at Berkeley performed beyond expectations. The faintest star which we identified with this photometer was  $10 \lambda$  Oph, an A1 star with  $m_v = 3.85$ . In Figure 7 we show a telemetry trace of the output of both the commercial and UC photometer. The UC photometer output (the lower trace) shows a scan through the horizon and two stars. The weaker star on this trace is  $23\beta$  Dra, a G2 star with  $m_v = 2.99$ . The trace on the original telemetry record clearly shows the thermal noise background of the photomultiplier tube employed in the photometer. The output of the commercial photometer (the upper trace) is shown for a 1st magnitude star for comparison. Note that for this photometer the background level is far above the thermal noise of the photocathode. In direct comparison, the UC photometer resolved stars a full magnitude fainter than the AS&E photometer in spite of the fact that it employed a smaller lens system.

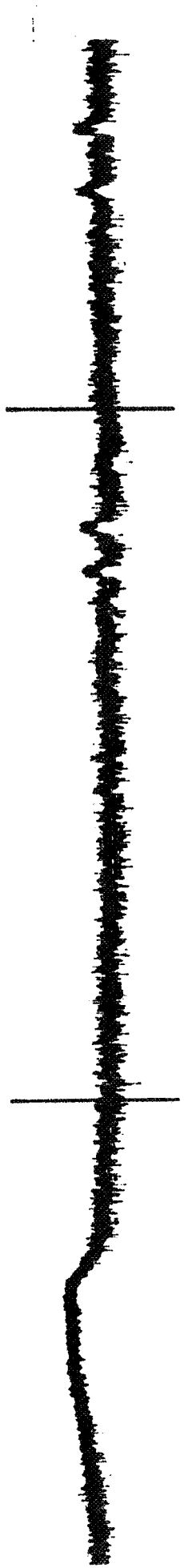


Figure 7. Comparison of stellar aspect signals from the University of California photometer (bottom trace) and a commercial unit.



## B. Development of a Balloon Gondola and X-ray Telescope

The development of a balloon borne gondola and large collecting area X-ray telescope, and two attempted flights with this system were described in an earlier report. As may be recalled, the instrumentation performed as expected but in the first attempted flight the balloon failed at launch and on the second attempt the balloon failed to reach observing attitudes. In spite of this discouraging beginning, we continued efforts to expand and improve this system.

At Spring and Fall upper wind turnaround, flights can be carried out which may last days. Because of solar heating, however, a balloon cannot remain at maximum altitude through a sunset unless substantial ballasting is carried out. For a large payload such as the one developed here, ballasting requirements are impractical. Hence the longest possible observing time for a single flight is 24 hours. In order to maximize the data from a single launch we decided to carry out subsequent flights only at the time of upper wind turnaround. Consequently we set as a design goal that the instrumentation should be operational for a minimum of twenty four hours. During this time the gondola should be oriented to  $\pm 1^\circ$ .

To achieve this goal we examined three different orientation methods.

### 1. A gas-jet system.

Laboratory tests plus results from our previous flight at about 100 K ft showed that good damping could be readily achieved with a gas thruster control. However this system had the following problems in regard to a 24 hour flight.

- a. Excessive consumption of gas, particularly as the system deadband was tightened up. Thruster duty cycle could not be more than 1-2% in order to permit 24 h operation. This was not attainable in the given circumstances, however, since a 10% duty cycle was required merely to hold against static swivel bearing friction.
  - b. Tendency to induce divergent modes of oscillating motion, especially at small deadband.
  - d. Logistic problems of high pressure gas storage and handling.
  - e. Difficulty in adjustment of thrusters to produce a perfect couple. Imperfect adjustment tended to induce unwanted motion which could become divergent.
2. Gas-jet system augmented by electrically driven swivel.

A large reduction in gas consumption could be realized with the use of an ideal (frictionless) suspension swivel. A "perfect" bearing could be synthesized by a servo-driven swivel operating in such a way as to hold the average value of the gas-jet error signal at zero. The gas jet system would then be used only for large scale orientation.

This is a good scheme in principle, but adds the complexity of two servo loops.

3. All-electric.

The use of an electric torque motor driving against the suspension line leads to a straight forward, simple and essentially linear servo loop. Gas logistics would be eliminated, as would the possibility of premature exhaustion of power.

Development was begun on an electric torque motor system. Electric power consumption was considered to be a problem due to the length of the flight contemplated and large amount of signal conditioning anticipated. Therefore, the ACS was designed to minimize power consumption. Since a torque motor output increases linearly with drive current while power increases as  $I^2$ , the motor should obviously be run at the lowest possible torque. The large moment of inertia of this payload, however, meant only a slow servo system was required. Accordingly, torque motor speed could readily be traded for torque, and this was done with a precision miniature roller chain coupling from motor to swivel. In the coupling developed the ratio is adjustable from 1:2.36 to 1:5.0 by changing the drive sprocket.

While the servo is ideally linear, swivel static friction introduces a discontinuity in the overall transfer junction that causes limit-cycling. This must obviously be much less than  $\pm 1^\circ$  pointing tolerance. The swivel bearing is therefore of utmost importance, since it sets the floor on servo performance. Upon evaluation of available swivel bearings it was decided to use a Miller Swivel Products, Inc. 2B swivel which has two full-complement angular contact ball bearings sharing the load. The swivel was disassembled, cleaned, and relubricated with Electromoly-48 low temperature grease (Electrofilm, Inc.) to render it operable at balloon altitude.

Work was also begun on optimizing the magnetometer stabilization loop. This work was continued under the subsequent grant to the University of California and a complete description of the system as modified will be provided in the final report of that grant.

C. Development of A Far UV Photometer for use in the Wavelength Band  
from 100 to 1000 Å

The results of this effort have been written up and submitted for publication. Since this work was supported solely by this contract and because this writeup covers this work in detail, we have included a preprint of this manuscript as Appendix I.

Appendix I

A Far Ultraviolet Photometer Far Space  
Research

A FAR ULTRAVIOLET PHOTOMETER FOR SPACE RESEARCH\*

(Short Title: Far U. V. Photometer)

C. STUART BOWYER AND FRANCESCO PARESCÉ

Department of Astronomy and Space Sciences Laboratory  
University of California, Berkeley

and

MICHAEL LAMPTON AND JOHN MACK

Space Sciences Laboratory  
University of California, Berkeley

Received \_\_\_\_\_

\*This work was supported by the National Aeronautics and  
Space Administration under grant NGR 05-003-278.

## ABSTRACT

A photometer for use in the wavelength region from 100 to 1300 Å has been developed. Specific bands within this region can be isolated by combining the spectral response of individual solar blind photocathodes with the transmission qualities of various thin metallic films. A continuous channel electron multiplier is used as a low background, high gain charge amplifier in the device. Each of these components are discussed in turn with emphasis placed on those characteristics which have special relevance to space borne instrumentation. Two examples of instruments employing these components are given, one a device to measure the resonantly scattered hydrogen and helium radiation in the upper atmosphere, and the other a device to measure the far UV photon flux generated in an aurora.

## INTRODUCTION

A number of programs in space research, both projected and in progress, involve the measurement of a low intensity, diffuse, far UV photon flux. The study of the earth's geocoronal hydrogen emission at  $1216 \text{ \AA}$  is undoubtedly the most well-known of these programs. Donahue (1966) has reviewed the extensive amount of work which has been carried out on this topic. Other areas of research in the far UV spectral region include the attempts of Byram et al. (1961), Bowyer et al. (1968), and Young et al. (1968) to measure the resonant helium emission at  $304 \text{ \AA}$  and  $584 \text{ \AA}$  from the earth's geocorona. Considerable effort has gone into the measurement of the far UV radiation produced in an aurora (Joki and Evans, 1969, and references cited therein). Information on the atmosphere of Venus (Barth et al. 1967) and Mars (Barth et al. 1969) has been obtained through the use of Lyman alpha detectors on planetary flybys. It has been suggested that the measurement of resonant helium emission from Jupiter is a means of defining the atmosphere of that planet (Bowyer et al., 1969; Judge, 1969). Bowyer and Lampton (1969) have suggested the use of a far ultraviolet photometer as a means of probing for a possible atmosphere on Mercury.

Most research in the far UV region of the spectrum has been carried out at wavelengths longward of the lithium fluoride



transmission cutoff at  $1050 \text{ \AA}$ . Typically an ionization chamber or photomultiplier is used as the primary detector. An alkali halide entrance window is used to define the shortwavelength cutoff of the device. In the case of the ionization chamber the long wavelength limit is set by the ionization potential of the gas while with photomultipliers this limit is determined by the work function of the photocathode.

The sun with its intense radiation flux is the only subject which has been studied in detail in the wavelength region between  $1050 \text{ \AA}$  and  $100 \text{ \AA}$ . The only attempts to measure a low intensity or diffuse flux at these wavelengths has been carried out in connection with the search for a possible geocoronal helium glow. This meager record has been due at least in part to the difficulty of carrying out even laboratory research at these wavelengths. These techniques have been slowly developed, however, and now the prime impediment to this type of work is the lack of instrumentation suitable for use in space.

A review of the work on the geocoronal helium glow illustrates the methods previously employed in this spectral region and points out their shortcomings. The first attempt to detect the night helium glow was made by Byram et al. (1961). They employed a windowless photo cell with a photoelectric surface of lithium fluoride. Although an upper limit for the

night helium glow was obtained using this device, it suffered from a number of shortcomings as a detector for this spectral region. The quantum efficiency of lithium fluoride as a function of wavelength has been measured by Samson (1967) and is shown in Figure 1. Since it has a substantial photoelectric yield over a broad range of wavelengths, relatively little spectral information can be obtained with this type of detector. As a device to measure the geocoronal helium glow, it suffers from the further shortcoming that the ratio of its quantum efficiency at  $584 \text{ \AA}$  to that at  $1216 \text{ \AA}$  is only about 150. Consequently, if the helium emission is less intense than the geocoronal Lyman alpha glow by a factor of 150 or more, a serious problem in source confusion results.

An additional problem with this type of detector is that it is extremely susceptible to particle contamination because of the lack of an entrance window. Low energy charged particles can be rejected electrostatically but this will not shield against neutral particles which could produce charged particles within the detector via secondary emission. Indeed, Byram et al. encountered a substantial background flux in flight which they attributed to metastable neutrals.

More recently, Bowyer et al. (1968) and then Young et al. (1968) employed a metallic filter/scintillator/photomultiplier detector in attempts to measure the night helium glow. In this detector a metallic filter on the order of  $1000 \text{ \AA}$  thick

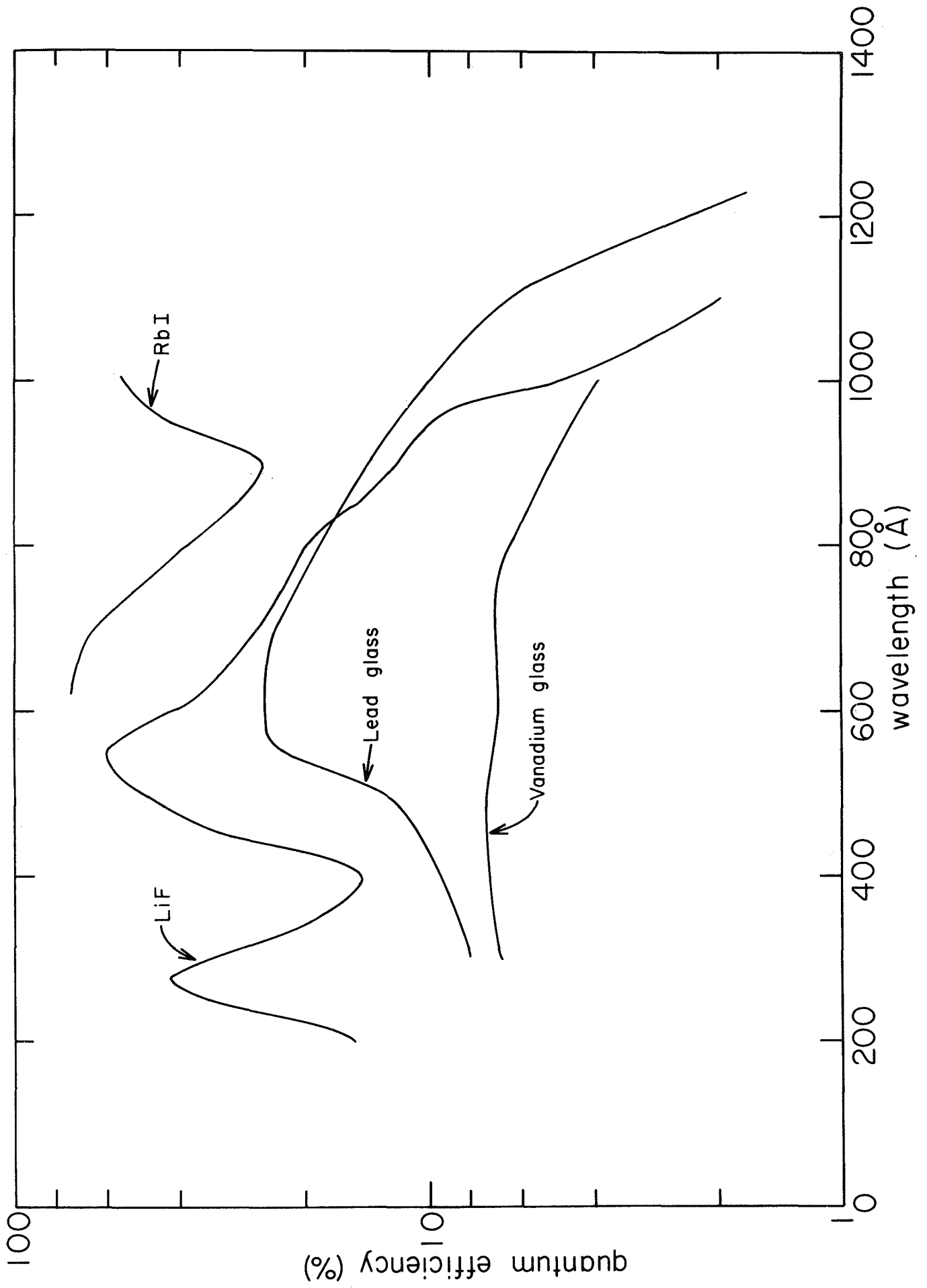


Figure 1. Far UV quantum yields of a number of photocathode materials.

is used as a bandpass filter to isolate the radiation of interest. The scintillator converts the desired radiation to optical photons which are then detected by the photomultiplier tube.

A number of problems were encountered by both groups with this type of detector. A primary problem was the detector's sensitivity to optical light. We found that even with perfect, newly made film-scintillator sandwiches these detectors were light-sensitive and hence suitable only for use at night. Under actual flight conditions this optical sensitivity severely compromised our intended measurement. Though the problem was much less severe in the experiment carried out by Young et al., the light sensitivity of their detector required that the data be subjected to a correction for optical background.

A second shortcoming of this type of detector is the problem of film degradation with time. The exact cause of this degradation has not been determined but it occurred in some cases with films which are stable when free standing. Consequently it may be the result of the prolonged intimate contact between the film and the scintillator material.

We have developed yet another far UV detector. The wavelength response of this device is determined by the spectral yield of a solar blind photoelectric surface in combination with the transmittance of a thin metallic film. A continuous

channel electron multiplier is employed as a low background charge amplifier allowing the detection of individual photon events.

#### DISCUSSION OF BASIC COMPONENTS OF THE DETECTOR

In the following we discuss in turn, charge amplification with the channel electron multiplier, photoelectric surfaces for far UV radiation, and the use of metallic films as spectral filters. Emphasis is placed on those characteristics which have special relevance to space-borne instrumentation.

##### A. The Channel Electron Multiplier

The channel multiplier has a number of distinct advantages as a charge amplifier for low-level signals and as a device for use in space instrumentation. Primary among these is its high gain allowing the detection of single photon events coupled with a very low background count rate. Other practical features are its compact size, low weight, electrical simplicity, low power requirements and ruggedness when properly mounted.

The continuous channel multiplier consists of a glass capillary tube bent to form a circular arc with an electron collector at one end to act as an anode. The capillary tube typically has an inner diameter of one to three millimeters. Either the glass itself is semiconducting or the inner surface of the capillary is treated to produce a semiconducting surface. If the capillary tube is made of semiconducting glass, it is found

that its resistivity is extremely temperature dependent. As a consequence, most channel multipliers are made from lead or vanadium doped glass. After being drawn into capillaries the glass is baked in a reducing atmosphere until a semiconducting surface is formed on the surface. The end-to-end resistance of the device is typically of the order of  $10^9$  ohms.

A potential difference is applied between the ends of the capillary which results in the establishment of a uniform electric field directed along the channel. A photoelectron introduced at the mouth of the channel is accelerated into the capillary by the electric field at the cathode. Upon colliding with the capillary wall, the electron liberates several secondary electrons which are in turn accelerated within the channel. Subsequent multiplications occur until either the electrons reach the anode or until space charge effects limit the pulse size. Channel multipliers are usually designed with sufficient length (3-5 cm) and are operated with sufficient voltage (3000 to 4000 V) that space charge phenomena dominate; under these conditions a typical pulse contains  $10^8$  electrons. At the anode end of the channel, an electrical connection serves to supply the current to the capillary and to couple pulses to the external circuitry.

The work function of the treated glass is of the order of three to four eV which is large compared to  $kT$ . As a

consequence, thermal noise does not contribute to the background of the device. The inner surface of the capillary is quite smooth and hence there is no field emission from this surface. Virtually the only contribution to the background of this device is that produced by cosmic rays. Cosmic rays can produce electrons within the capillary and if this occurs near the cathode sufficient multiplication will take place to produce a background count. This background is not large because of the small cross-sectional area of the capillary. Consequently typical background count rates for channel multipliers are on the order of  $10^{-2}$  counts/sec.

Because of the large photon and particle fluxes which may be encountered by any space instrumentation, it is important to examine the response of the channel multiplier to large count rates and to establish a lower limit on total counts which it can accommodate. The instantaneous count rate is limited by the loss of electrons from the channel wall during a signal pulse. This charge must be supplied by the channel conductance which must reestablish the initial distribution of electrical potential along the tube. The time constant for this to occur is the product of the channel resistance and the channel capacity, which typically is about  $10^{-4}$  seconds. Because the pulses are themselves limited in charge, the potential distribution will not be seriously upset if  $\Delta I \cdot R \ll V_s$

where  $\Delta I$  is the average current due to pulses of charge  $Q$  occurring at frequency  $f$ ,  $R$  is the channel resistance, and  $V_s$  the total potential drop along the channel. This requires only that  $f \ll I_{dc}/Q = 3 \times 10^5$  counts/second. At greater count rates the redistribution of electric field within the channel diminishes the charge available within each pulse. Typical amplifiers and discriminators used with channel multipliers permit counting events having  $Q$  as small as  $10^5$  electrons. Consequently the practical maximum count rate is often determined not by the channel multiplier itself but rather by the resolving time of the amplifier-discriminator combination. Under optimum conditions Wolber et al. (1969) have been able to resolve pulses spaced  $5 \times 10^{-8}$  seconds apart. Hence providing the input pulses have a Poisson distribution in arrival times, less than 1% of the incident counts will be missed at counting rates of  $5 \times 10^6$  counts per second or less.

A number of studies have been carried out to determine if there is a limitation on the total accumulated counts which a channel multiplier can detect. These studies were prompted by the observation that the gain of this device can vary with a number of parameters (McCullough, 1968; Wolber et al., 1969; Reed et al. 1969). It is found that the gain of a multiplier which has been exposed to air decreases by a factor of two or



three until an accumulated count of  $10^7$  to  $10^8$  is reached, after which the gain is constant for a given count rate. This change is attributed to the removal of surface layers of gas from the interior of the multiplier by electron bombardment. It has also been established that the gain of a channel multiplier is dependent upon the counting rate and typically varies by a factor of two over a change in count rate from 0 to  $10^4$  counts per second. This change is reversible, however, and the gain is found to return to its initial value when the count rate is reduced. Though it has not been definitely established, there is some evidence that a long-term gain loss occurs with very large numbers of accumulated counts. This effect does not occur with total accumulated counts of  $10^{11}$  or less, however.

Channel multipliers have been employed for the measurement of charged particle fluxes on a number of spacecraft. The University of Iowa detector is typical of these instruments and is described in the literature (Frank, 1967a; Frank 1967b); similar instruments have been used successfully on OGO-3 and also the IMP-4 and Injun satellites. Over two years of continuous data coverage has been obtained with these instruments and verify that, given care in selecting and preparing the device, at least  $10^{11}$  counts can be obtained with this device in a space environment without impaired gain or efficiency (Frank, 1969).

## B. Photocathode Surfaces

A number of photocathode surfaces have been considered for use with this detector. Various alkali halides, metals, and the conductive glass of the channel electron multiplier itself all have the advantage of a relatively high quantum yield in the far UV coupled with a low yield outside this band.

Metzger (1965) determined the quantum yield of twenty alkali halides in the far UV. These compounds have the highest quantum yields of any of the materials we have considered. Unfortunately most alkali halides are deliquescent and must be treated with care. Lithium fluoride is an example of an alkali halide which has a spectral response which is potentially quite useful. Although it must be protected from moisture, it has nonetheless been used extensively in space research. Unfortunately, no studies have been made on the long term stability of the quantum yield of this material under conditions typical of a prelaunch environment. The quantum yield of rubidium iodide is shown in Figure 1 (after Metzger, 1965) as a second example of a photocathode whose response would be especially useful for particular far UV studies.

The semiconducting glass of the channel multiplier can be used as the photocathode for this detector. Timothy et al. (1967) have measured the quantum yield of vanadium doped channel multiplier glass over the range from 500 to 1300 Å and Johnson (1969) has measured the quantum efficiency of lead doped channel multiplier glass in the range from 300 to 1000 Å. Their results

are reproduced in Figure 1. We have limited our studies to the lead doped glass in view of its substantially higher quantum yield over the region of interest. We have measured the quantum efficiency of this material at  $304 \text{ \AA}$  and have also measured the response of this material to X-rays at two different energies. The X-ray measurements were necessary to determine the response of the photocathode to the universal X-ray background flux. The  $304 \text{ \AA}$  measurement was carried out with a grazing incidence spectrometer similar to that described by Landon (1966). A hollow cathode discharge tube was used as a source and a gold foil photodiode was used as a standard detector for this measurement. The quantum efficiency of gold at this wavelength has been measured by Cairns and Samson (1966). The X-ray measurements were carried out with the use of  $\text{Fe}^{55}$  and  $\text{Cd}^{109}$  radioactive sources which produce 5.9 and 22 keV photons respectively. The absolute intensity of the  $\text{Fe}^{55}$  source was measured with a proportional counter and the intensity of the cadmium source was measured with a scintillator/photomultiplier detector. The results of these measurements are given in Table 1. The  $304 \text{ \AA}$  measurement has been added to the data shown in Figure 1.

Johnson (1968) measured the stability of the photoelectric yield of lead doped channel multiplier glass when subjected to exposure to the atmosphere and to water vapor. He found that the yield did not vary by more than a few percent over the test

period involved. Interestingly enough, the limiting factor on the accuracy of this experiment appeared to be a drift in the nitric oxide calibration detector employed.

The photoelectric yields of a large number of metals have been measured and these have been compiled by Samson (1967). These yields are not as high as that of the alkali halides or of semiconductive lead glass but they are still quite substantial. Madden (1969) has carried out an extensive study of the long term stability of the photoelectric yield of tungsten, gold, chromium and aluminum at  $584 \text{ \AA}$ . He found that the quantum efficiency of these materials were stable to within 1 to 5% over the five-month lifetime of the test. While these materials would be suitable for use in the instrumentation described herein, they seem to offer no special advantages over a photocathode constructed of treated lead glass.

### C. Thin Metallic Filters

Thin metallic films are virtually the only materials which can be used as spectral filters in the far UV. The fabrication of these films has been discussed in the literature (see, for example, Vouros et al. 1968). Typically they are made by evaporating the desired metal onto a glass substrate which has been coated with a parting agent. The films are removed from the substrate by soaking in distilled water. After drying, the films are epoxied onto an electroformed mesh backing and mounted

in a holder. Films made in this manner are surprisingly rugged. We have tested 1000 Å aluminum films and found they will withstand pressure differentials of well over 10 mm Hg without failure. The pinhole transmission of such a film can readily be made as low as 1 part in  $10^8$ .

To a first approximation one can treat the transmission of electromagnetic radiation by a thin metallic film as if the electrons in the film were a plasma. The critical plasma frequency for a typical metal falls in the far UV. Below this frequency the metal will reflect electromagnetic radiation while above it the material will be transparent. A complete analysis is complex and in reality transmission is observed only over a narrow range of frequencies. A substantial amount of experimental work has been carried out on the transmission of thin metallic foils to far UV radiation. Samson (1967) has assembled a large amount of these data. A cursory examination of this work shows that a wide range of possibilities exists for isolating different bands within the far UV wavelength region.

The most obvious applications for the detector described here concern the measurement of the 304 Å line of singly ionized helium, the 584 Å line of neutral helium and the Lyman beta line of hydrogen at 1024 Å. In Figure 2 we show the transmittance of a number of films which are potentially useful for this type of work. The values for aluminum, tin and indium are from Hunter et al. (1965) and those for carbon are from Samson and Cairns (1966).

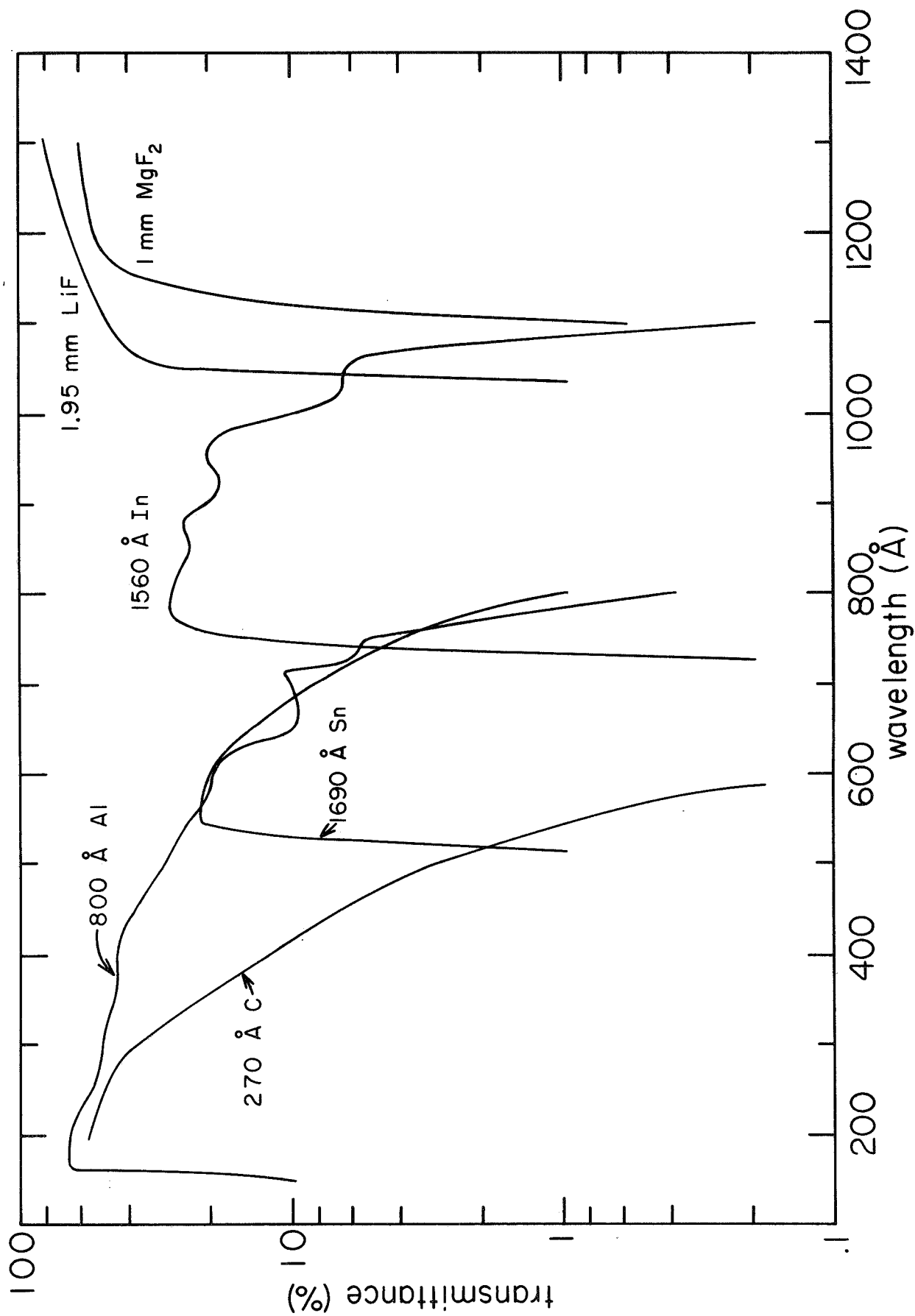


Figure 2. Far UV transmittance of selected metallic films.

We have considered the use of a carbon film to isolate a band about the 304 He II line. A thin carbon film has a high transmission at 304 Å but is virtually opaque at 584 Å. Since these films are quite fragile, we have coated approximately 300 Å of carbon onto 1100 Å thick aluminum films. The result is a filter which is quite strong, and highly selective for 304 Å radiation. We have stored films of this type in our laboratory for over six months and have observed no change in their physical characteristics.

An examination of the data compiled by Samson suggests that a 2000 Å film of bismuth would provide a means of isolating the 584 He I line. We have found, however, that films of this material oxidize relatively rapidly and that after a period of several months they are no longer usable. We have also tried a combination of tin and aluminum to isolate the 584 Å line. Here we hoped to combine the proved strength of the aluminum film with the bandpass qualities of tin. Unfortunately, tin and aluminum form an intermetallic compound. The electronic band structure of the intermetallic is different from that of the metals themselves and consequently the far UV transmission is also different.

As can be seen from the data in Figure 2, tin films have ideal bandpass properties for studying the 584 He I radiation and indium films would be suitable for isolating the 1024 Å

Lyman beta line of hydrogen. A drawback to both of these films is that their grain boundaries grow with time and eventually reach a size where pinholes are produced. Typically a good quality film made from these materials will have a pinhole transmission of  $10^{-8}$  when first fabricated but will deteriorate until a transmission of  $10^{-5}$  is reached. Thereafter the film will remain stable. Consequently if these films are to be used in an instrument, either the experiment must be able to tolerate a  $10^{-5}$  pinhole transmission or two films must be used in series with a resultant loss in overall transmission.

We have included data on the transmittance of lithium fluoride and magnesium fluoride in Figure 2. Either of these materials could be used as a filter to provide a detector for the hydrogen Lyman alpha line. Heath and Sacher (1966) have shown that the transmittance of lithium fluoride degrades severely under irradiation by 1 to 2 MeV electrons while the transmittance of magnesium fluoride does not. Consequently for a detector which is expected to encounter a high radiation environment, the magnesium fluoride window would be clearly preferable.

#### SPECIFIC INSTRUMENTATION

We have developed two instruments employing these basic components. The first of these is designed to measure resonantly scattered far UV radiation in the upper atmosphere. The



complete instrument consists of a high voltage power supply, a channel multiplier, a thin metallic filter, a charge sensitive amplifier and a temperature compensated logarithmic rate-meter. The packaging for these components is quite straightforward. We have used a variety of metallic filters in this configuration in an attempt to isolate the 304, 584 and 1024 Å lines of helium and hydrogen. Typical bandpasses of the filter/photocathode combinations employed are shown in Figure 3. The response of a given instrument will depend upon the individual photocathode and the specific thickness of the filter employed. The measured response of three of these detectors at a number of wavelengths is given in Table II.

At sounding rocket altitudes, charged particles would not be expected to produce a background in this type of detector since a thousand Angstrom metal film will stop electrons with energies up to about 2 keV. We have found, however, that at least under some conditions a small charged particle background does exist at these altitudes. Consequently we have added a small magnetic broom which in combination with a drilled hole collimator is capable of excluding electrons with energies up to several hundred keV.

This instrument is shown on the left in Figure 4. In Table III we list a few of the overall parameters of the instrument.

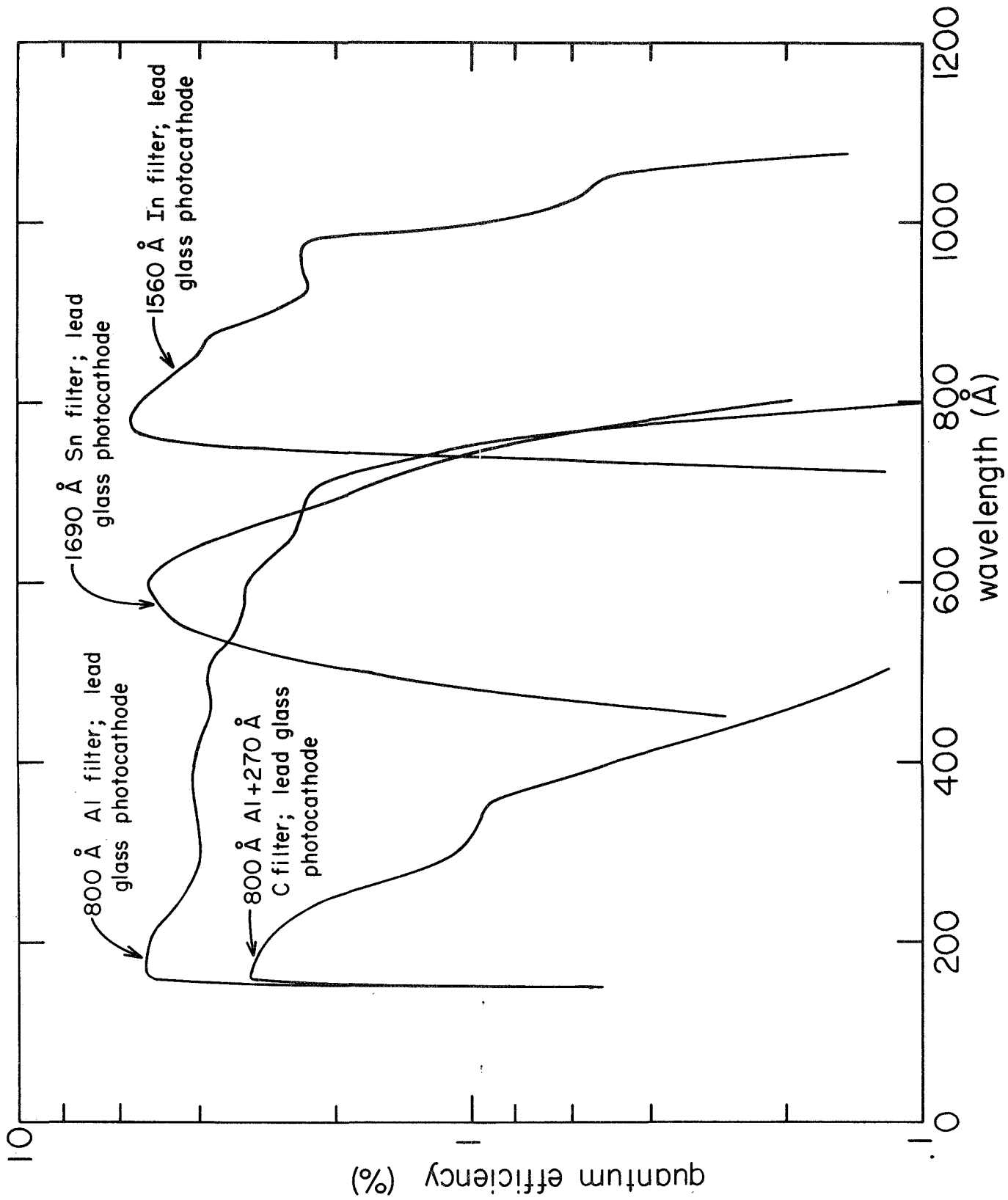


Figure 3. Detection efficiencies of a number of metallic filter/lead glass phototocathode combinations.

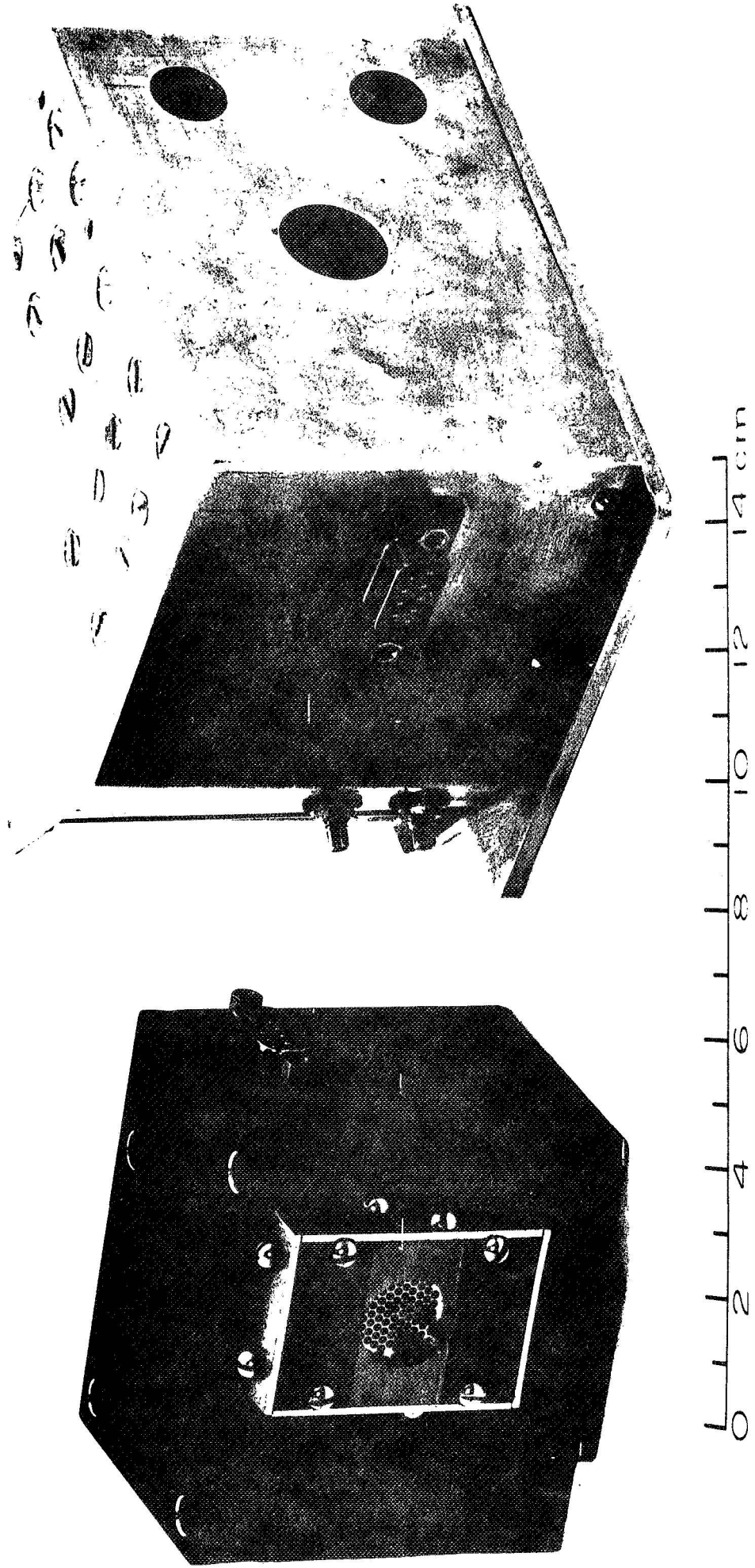
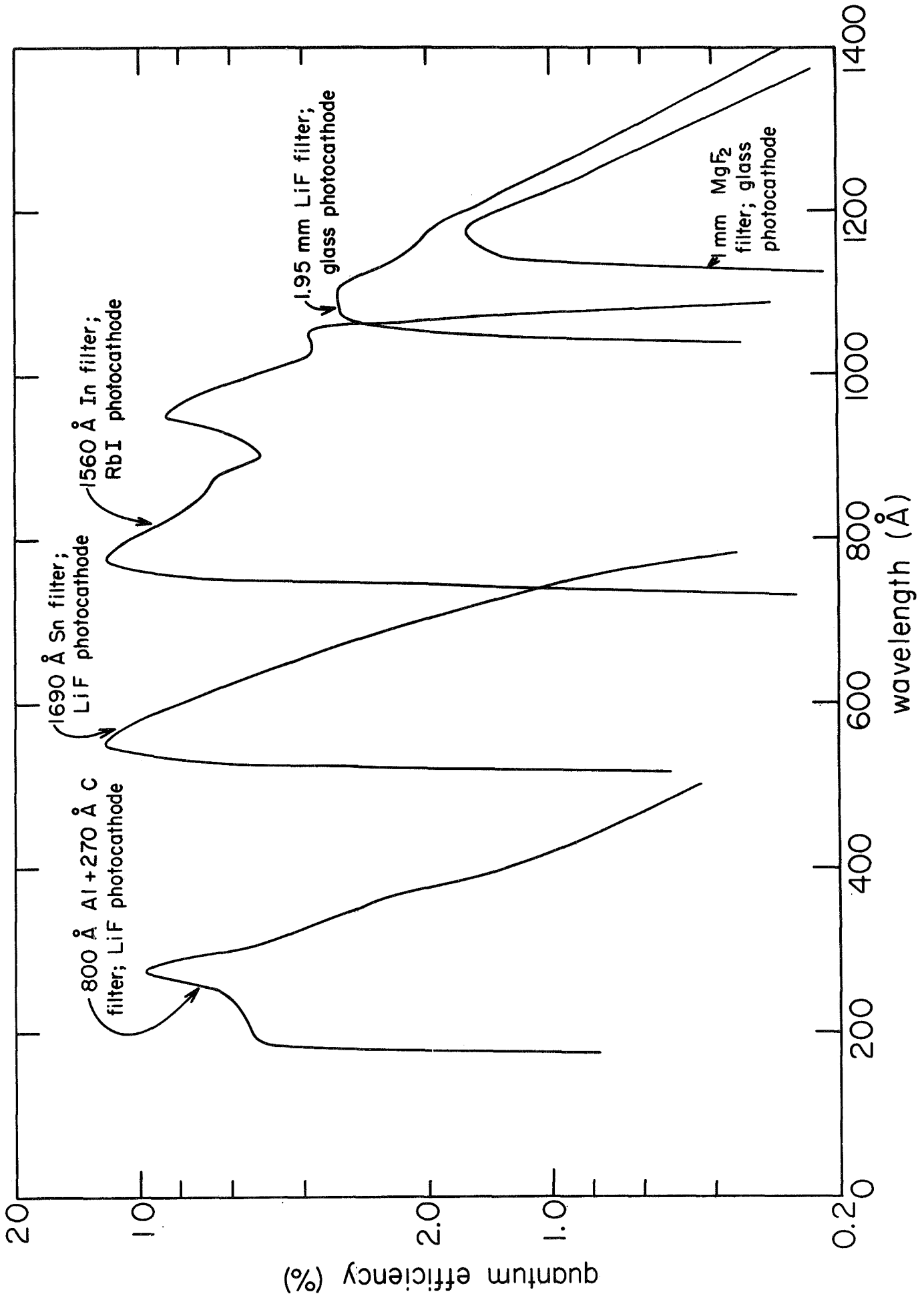


Figure 4. Far UV photometers developed for atmosphere and auroral studies.

In Figure 5 we show the theoretical detection efficiencies of some filter/photocathode combinations which at least in principle are more efficient for this type of work. The increase in efficiency varies from a factor of two at  $584 \text{ \AA}$  to a factor of seven for Lyman beta radiation. The usefulness of these detectors depends, of course, on the degree of stability of the individual alkaline halide used as the photocathode. We also show in Figure 5 the overall detection efficiency of a hypothetical Lyman alpha detector employing either a magnesium fluoride or lithium fluoride window. While such a combination isolates a wavelength band about  $1216 \text{ \AA}$ , the detection efficiency at this wavelength is substantially less than that which can be achieved with an ion chamber or photomultiplier.

A second device we have built employing these components is intended for use in auroral studies. The design of this instrument is greatly complicated by the necessity of carrying out this measurement in the presence of a flux of energetic particles, both charged and neutral. The charged particles can easily be eliminated by a magnetic broom. The neutrals will obviously not be removed by this device and a significant fraction of these will undergo charge exchange in passing through the metallic filter. Even if a second magnet were employed to remove these ions, the neutrals themselves would be sufficiently energetic to be detected via secondary

Figure 5. Theoretical detection efficiencies of some filter/photocathode combinations desirable for studies of resonantly scattered radiation in the earth's upper atmosphere.



emission at the photocathode. An alternate possibility for removing the particle flux would be to employ a mirror which would reflect the UV but not the particles. The only materials effective as reflectors for far UV radiation, however, are metals with high atomic numbers, and these are also effective at scattering electrons.

The detection scheme finally devised is outlined in Figure 6. An 800 Gauss magnetic field removes charged particles from the incident beam. A platinum mirror surface absorbs the neutral particles and reflects the UV to the filter/photocathode. On a relative basis platinum has one of the highest reflection coefficients in the far UV. Nonetheless on an absolute scale its reflection coefficient is not large and hence with the introduction of the mirror the overall detection efficiency of the device is substantially reduced. Fortunately this is not a serious problem for auroral studies since the UV fluxes expected are on the order of hundreds of Rayleighs. In Table IV we have listed the measured detection efficiencies of two of these instruments at several wavelengths.

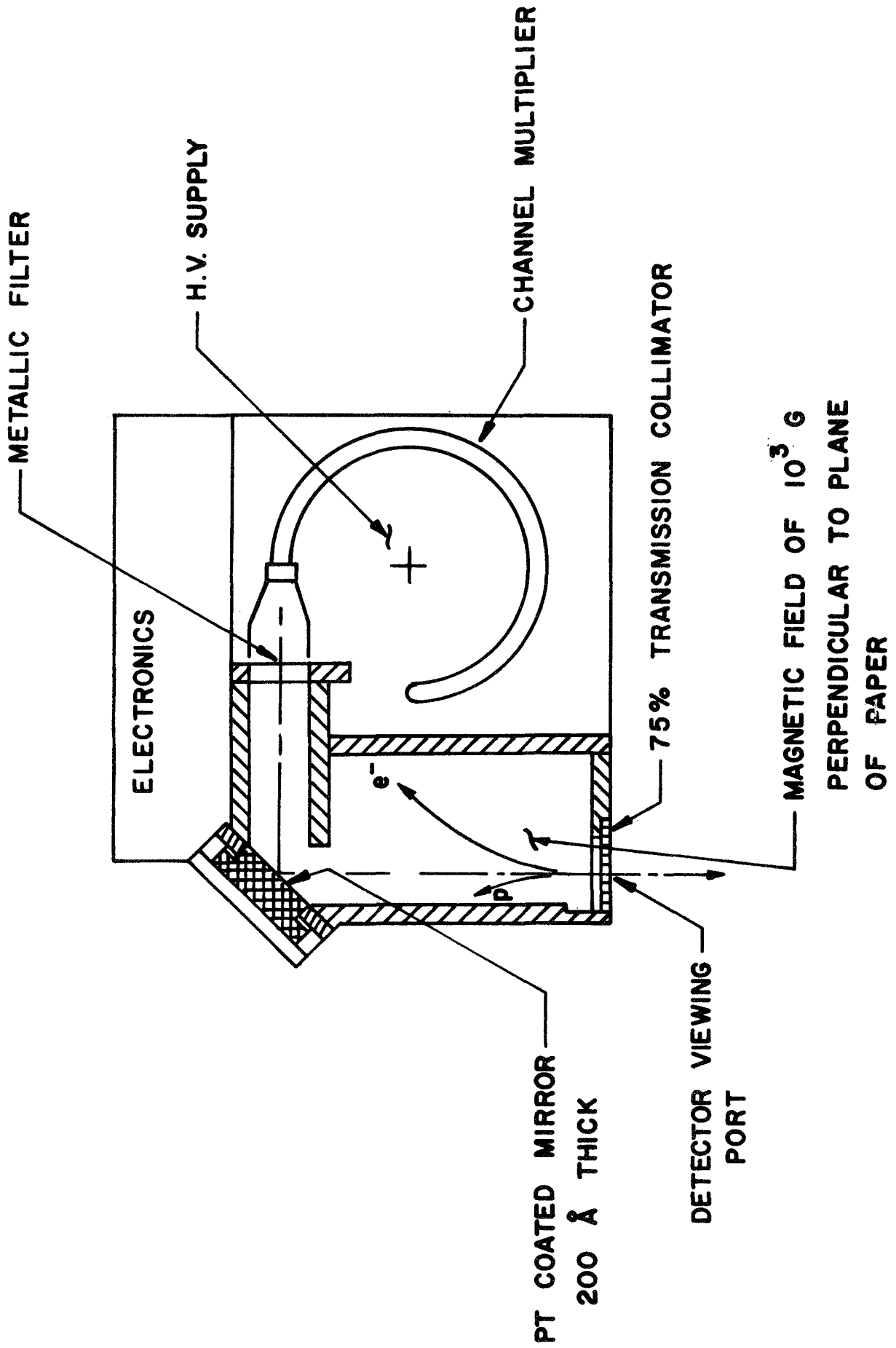


Figure 6. Charged particle rejection scheme employed in a far UV photometer to be used in auroral studies.

We have measured the charged particle response of this instrument with an electrostatic accelerator. Fluxes of  $10^6$  electrons/sec,  $5 \times 10^5$  protons/sec and  $2 \times 10^5$  neutrals/sec were directed in turn at the aperture of the detector. The energy of these particles was varied continuously from 0 to 60 keV. At no point in this test sequence did the background count rate exceed 4 counts/sec.

The instrument shown on the right in Figure 4 contains two of these detectors which were packaged in a single housing for convenience. This unit weighs three pounds and uses slightly more than one watt of power.

#### CONCLUSIONS

A detector covering the range from 100 to  $1300 \text{ \AA}$  which is suitable for space research has been developed. Relatively narrow spectral regions within this range can be isolated to study lines of special geophysical or astrophysical interest. The components used in this detection scheme are small, rugged, stable and require little power for operation.

We have developed two different instruments employing these components, one for studies of the resonantly scattered far UV radiation in the earth's upper atmosphere and the other for studies of UV emission in auroras. In addition, we expect that this device will find wide applicability in other programs in space research.



## ACKNOWLEDGMENTS

We would like to thank Mr. Gordon Steele for many informative discussions concerning thin metallic films.

## REFERENCES

- Barth, C. A., W. G. Fastie, C. W. Herd, J. B. Pearce, K. K. Kelly, A. I. Stewart, G. E. Thomas, G. P. Anderson, and O. F. Raper, Science, 165, 1004 (1969).
- Barth, C. A., J. B. Pearce, K. K. Kelley, L. Wallace, and W. G. Fastie, Science, 158, 1675 (1967).
- Bowyer, C. S., P. M. Livingston, and R. Price, J. Geophys. Res., 73, 1107 (1968).
- Bowyer, C. S., M. Lampton, G. B. Field, I. Axford, and H. Spinrad, Proposal to Measure the Resonant Helium Emission from the Atmosphere of Jupiter, Submitted to NASA (1969).
- Bowyer, C. S., and M. Lampton, Proposal for a Broad Band Ultraviolet Spectrometer to Measure the Atmosphere of Mercury, Submitted to NASA (1969).
- Byram, E. T., T. A. Chubb and H. Friedman, J. Geophys. Res., 66, 2095 (1961).
- Cairns, R. B., and J. A. R. Samson, J. Opt. Soc. Amer., 56, 1568 (1966).
- Donahue, T. M., Annales de Geophysique, 22, 175 (1966).
- Frank, L. A., J. Geophys. Res., 72, 185 (1967a).
- \_\_\_\_\_ , J. Geophys. Res., 72, 3753 (1967b).
- \_\_\_\_\_ , Private Communication (1969).

- Heath, D. F., and P. A. Sacher, Appl. Optics, 5, 937 (1966).
- Hunter, W. R., D. W. Angel, and R. Tousey, Appl. Optics, 4, 891 (1965).
- Johnson, M. C., Review of Scientific Inst., 40, 311 (1969).
- Joki, E. G., and J. E. Evans, J. Geophys. Res., 74, 4677 (1969).
- Judge, D. L., Proposal to Measure the Resonant Helium Emission from Jupiter, Submitted to NASA (1969).
- Landon, D. O., Appl. Optics, 3, 115 (1964).
- Madden, R. P., National Bureau of Standards Internal Report (1969).
- Metzger, P. H., J. Phys. Chem. Solids, 26, 1879 (1965).
- Samson, J. A. R., Tech. of Vacuum Ultraviolet Spectroscopy, Wiley, New York (1967).
- Samson, J. A. R., and R. B. Cairns, Appl. Optics, 4, 915 (1965).
- Timothy, A. F., J. G. Timothy, and A. P. Willmore, Appl. Optics, 6, 1319 (1967).
- Vouros, P., J. I. Masters, and R. J. Starble, Rev. Scient. Inst., 39, 741 (1968).
- Wolber, W. G., B. D. Klettke, J. S. Miller, and K. C. Schmidt, to be published in Appl. Phys. Letters, 1969.
- Young, J. M., G. R. Carruthers, J. C. Holmes, C. Y. Johnson, and N. P. Patterson, Science, 160, 990 (1968).

TABLE I

---

<u>Wavelength (energy)</u>	<u>Quantum Efficiency</u>
304 Å (40.8 eV)	8 %
2.1 Å (5.9 keV)	4 %
.56 Å (22 keV)	1.2%

---

TABLE II

Atmospheric Photometer Detection Efficiencies (in %)

---

	Al Filter	Al+C Filter	In Filter
304 Å	3	2.5	--
584 Å	2	0.1	--
1025 Å	$4 \times 10^{-4}$	$8 \times 10^{-5}$	.4
1216 Å	$8 \times 10^{-5}$	$1.5 \times 10^{-6}$	--

---

TABLE III

## Physical Parameters of the Atmospheric Photometer

---

Size	3" x 2 $\frac{1}{2}$ " x 2"
Weight	1.2 lbs
Power Consumption	1.3 Watts
Effective Photocathode	0.7 sq. cm
Solid Angle (Typ.)	0.028 steradians

---

TABLE IV

Auroral Photometer Detection Efficiency (in %)

---

	Al+C Filter	Al+Sn Filter
304 Å	$6 \times 10^{-2}$	$4 \times 10^{-2}$
584 Å	$4 \times 10^{-3}$	$1.1 \times 10^{-1}$
1216 Å	$1.5 \times 10^{-6}$	$1.5 \times 10^{-4}$

---